

Crystal Engineering of Stacked Aromatic Columns. Three-Dimensional Control of the Alignment of Orthogonal Aromatic Triads and Guest Quinones via Self-Assembly of Hydrogen-Bonded Networks

Yasuhiro Aoyama,^{*,†} Ken Endo,[†] Takashi Anzai,[‡] Yuji Yamaguchi,[‡]
Tomoya Sawaki,[‡] Kenji Kobayashi,[‡] Nobuko Kanehisa,[§] Hiroshi Hashimoto,[§]
Yasushi Kai,^{§,1} and Hideki Masuda^{1,2}

Contribution from the Institute for Fundamental Research of Organic Chemistry, Kyushu University, Hakozaki, Higashi-ku, Fukuoka 812-81, Japan, Section of Biofunctional Chemistry, Department of BioEngineering, Nagaoka University of Technology, Kamitomioka 940-21, Japan, Department of Applied Chemistry, Osaka University, Yamadaoka, Suita 565, Japan, and Department of Applied Chemistry, Nagoya Institute of Technology, Gokiso-cho, Showa-ku, Nagoya 466, Japan

Received October 27, 1995. Revised Manuscript Received March 20, 1996[⊗]

Abstract: We here determined the crystal structures of several adducts of the bis(resorcinol) and bis(pyrimidine) derivatives of anthracene or anthraquinone (**1–3**) as orthogonal aromatic triads. Anthracene-bis(resorcinol) compound **1** forms molecular sheets consisting of hydrogen-bonded homopolymeric chains of resorcinol together with anthracene stack columns having a face-to-face distance of $I_{a-a}^f = 12.0\text{--}13.4 \text{ \AA}$; large supramolecular cavities left are occupied by two solvent molecules as guests via hydrogen bonding. Cocrystallization of compound **1** with anthracene-bis(pyrimidine) derivative **2** affords adduct **1·2**, whose molecular sheets are composed of hydrogen-bonded resorcinol-pyrimidine alternate copolymeric chains and closer anthracene columns with $I_{a-a}^f = 8.40$ or 8.49 \AA . Columns in neighboring sheets are in a close proximity or even partially overlapped as a result of interpenetration of the sheets. Compound **1** also forms a 1:1 adduct with anthraquinone-bis(pyrimidine) derivative **3**. The resulting adduct **1·3** exclusively forms a resorcinol-pyrimidine O–H···N hydrogen-bonded network as above but in a different way. The resulting sheets are layered so as to give segregated columns of anthracene ($I_{a-a}^f = 11.78 \text{ \AA}$) and anthraquinone ($I_{q-q}^f = 10.56 \text{ \AA}$) which are partially overlapped with each other. Compound **1** and quinone form 1:2 (**1** to quinone) adducts. An extensive **1**-quinone hydrogen-bonded network in the benzoquinone adduct leads to 3-fold interpenetrating or polycatenating molecular sheets having highly slided anthracene columns ($I_{a-a}^f = 3.99 \text{ \AA}$) and quinone columns ($I_{q-q}^f = 2.87 \text{ \AA}$). The anthraquinone adduct, on the other hand, forms hydrogen-bonded one-dimensional alternate chains composed of **1** and face-to-face stacked quinone dimer. These chains are so arranged as to give segregated and partially overlapped columns for anthracene ($I_{a-a}^f = 5.24 \text{ \AA}$) and anthraquinone ($I_{q-q}^f = 3.03$ or 3.55 \AA). It is remarkable that many of the columns are constructed via self-assembly of hydrogen-bonded one-dimensional (1D) or two-dimensional (2D) networks. The *network-self-assembly strategy* thus opens the door to a three-dimensional (3D) control of aromatic columns in molecular crystals, i.e., co-alignment in proximity of donor columns and acceptor columns.

Introduction

Design of crystal structures is still a tough challenge in materials science and technology.³ Manipulation of functional aromatic and heteroaromatic stack columns is an especially intriguing target in view of their potential electronic and photoelectronic properties; highly conducting or superconducting organic materials, for example, generally possess such a structure.⁴

Directed hydrogen-bonding has often been used to restrict

mutual arrangement of molecules in crystals.⁵ Recently, we have proposed what we call the orthogonal aromatic-triad strategy.⁶ The essential point of this lies in the orthogonal arrangement of a function-responsible aromatic spacer (S) and interaction-responsible aromatic rings. A bis(resorcinol) derivative of anthracene (**1**, Scheme 1) forms an extensive hydrogen-bonded network similar to that shown in Figure 1a (X = Y = OH and S = S' = anthracene), thereby forcing the *orthogonal*

[†] Kyushu University.

[‡] Nagaoka University of Technology.

[§] Osaka University.

¹ Nagoya Institute of Technology.

[⊗] Abstract published in *Advance ACS Abstracts*, May 15, 1996.

(1) Responsible for the crystal structure determination carried out in Osaka University for adduct **1·2** and **1·3**·C₆H₅OCH₃.

(2) Responsible for the crystal structure determination carried out in Nagoya Institute of Technology for adducts **1·2BQ** and **1·2AQ**.

(3) (a) Kitaigorodskii, A. I. *Molecular Crystals and Molecules*; Academic Press: New York, 1973. (b) Wright, J. D. *Molecular Crystals*; Cambridge University Press: Cambridge, 1987. (c) Desiraju, G. R. *Crystal Engineering: The Design of Organic Solids*; Elsevier: New York, 1989.

(4) (a) Phillips, T. E.; Kistenmacher, T. J.; Ferraris, J. P.; Cowan, D. O. *J. Chem. Soc., Chem. Commun.* **1973**, 471–472. (b) Bechgaard, K.; Jacobsen, C. S.; Mortensen, K.; Pedersen, H. J.; Thorup, N. *Solid State Commun.* **1980**, *33*, 1119–1125. (c) Jérôme, D.; Mazaud, A.; Ribault, M.; Bechgaard, K. *J. Phys. Lett. (Orsay, Fr.)* **1980**, *41*, 95–98. (d) Thorup, N.; Rindorf, G.; Soling, H.; Bechgaard, K. *Acta Crystallogr.* **1981**, *B37*, 1236–1240. (e) Jacobsen, C. S.; Tanner, D. B.; Bechgaard, K. *Phys. Rev. Lett.* **1981**, *46*, 1142–1145.

(5) MacDonald, J. C.; Whitesides, G. M. *Chem. Rev.* **1994**, *94*, 2383–2420 and references cited therein.

(6) (a) Kobayashi, K.; Endo, K.; Aoyama, Y.; Masuda, H. *Tetrahedron Lett.* **1993**, *34*, 7929–7932. (b) Aoyama, Y.; Endo, K.; Kobayashi, K.; Masuda, H. *Supramolecular Chem.* **1995**, *4*, 229–241. (c) Endo, K.; Sawaki, T.; Koyanagi, M.; Kobayashi, K.; Masuda, H.; Aoyama, Y. *J. Am. Chem. Soc.* **1995**, *117*, 8341–8352.

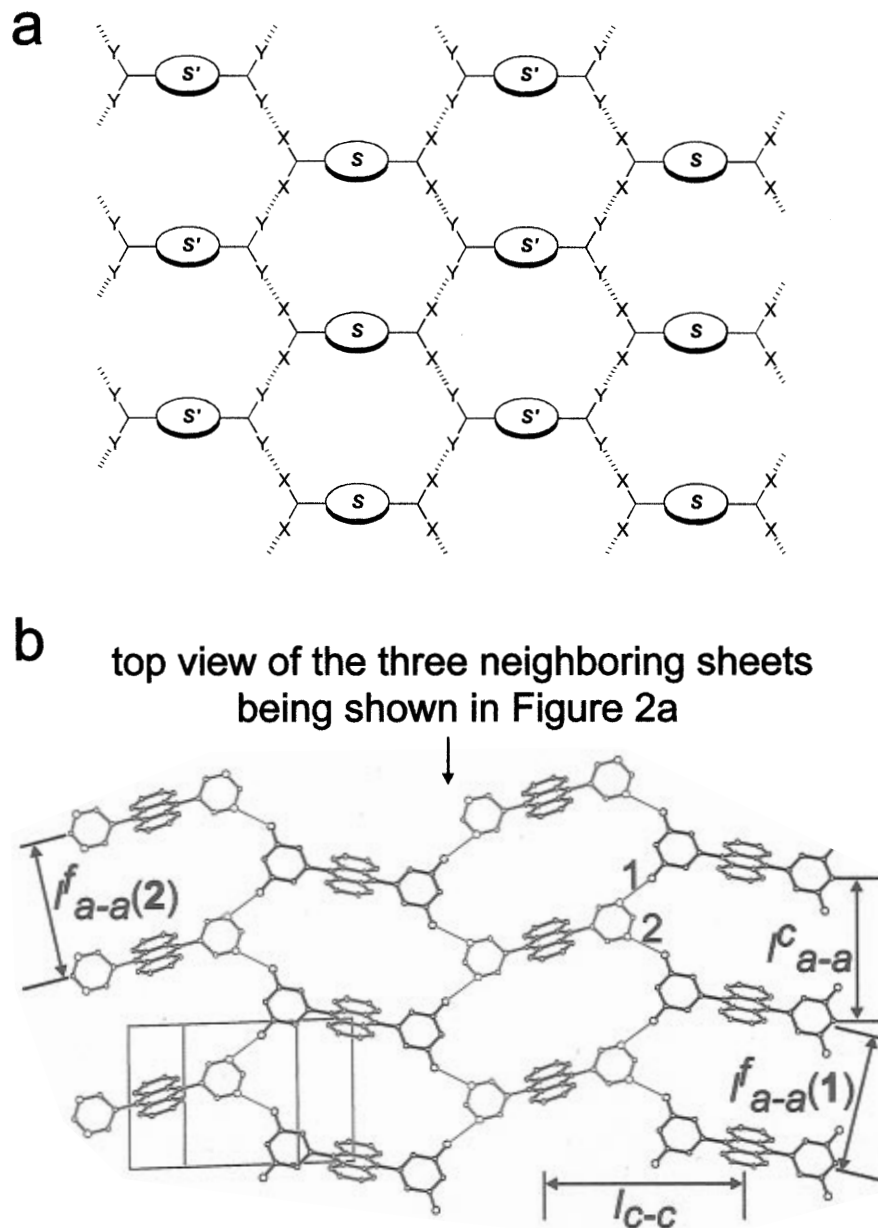
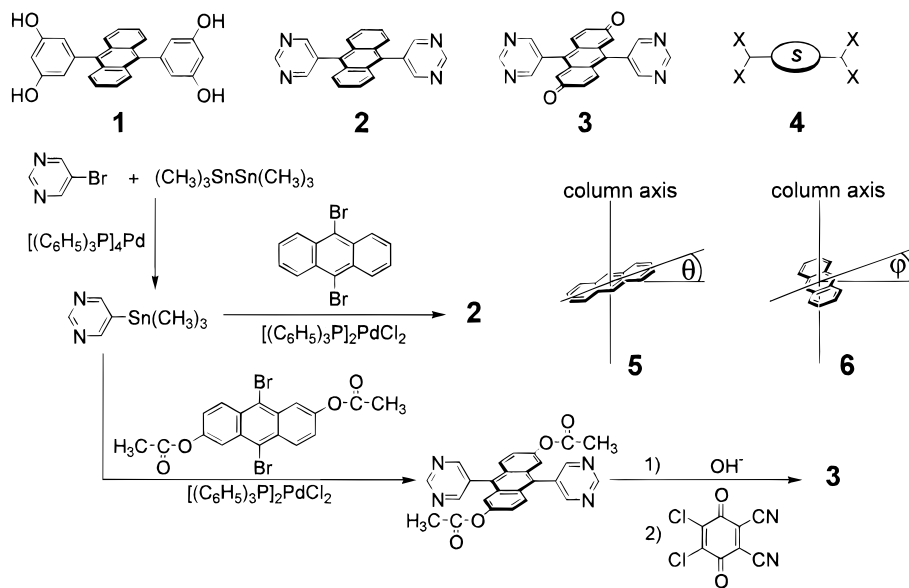
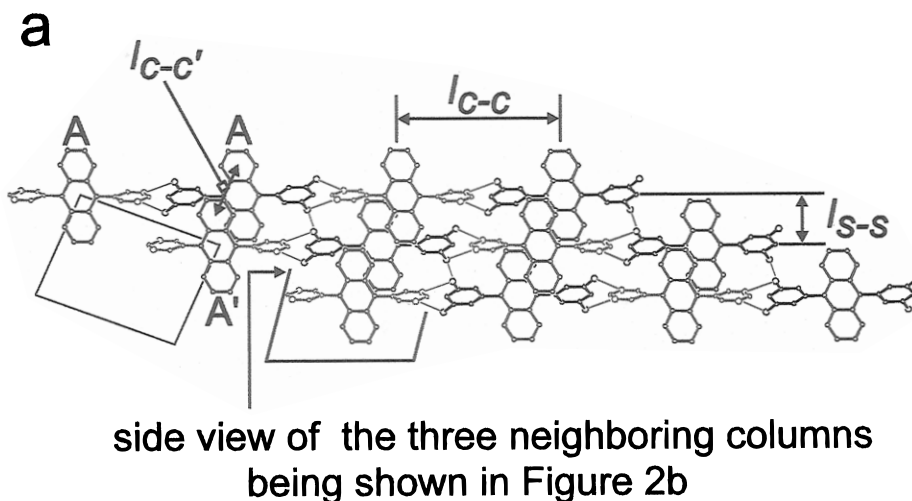


Figure 1. Structure of the hydrogen-bonded network in a molecular sheet in the crystal of adduct **1·2**: schematic representation (a) and actual structure (b), where anthracene, resorcinol, and pyrimidine rings are shown in red, black, and blue, respectively, and hydrogen bonds are in light blue.

Scheme 1





b (stereoview)

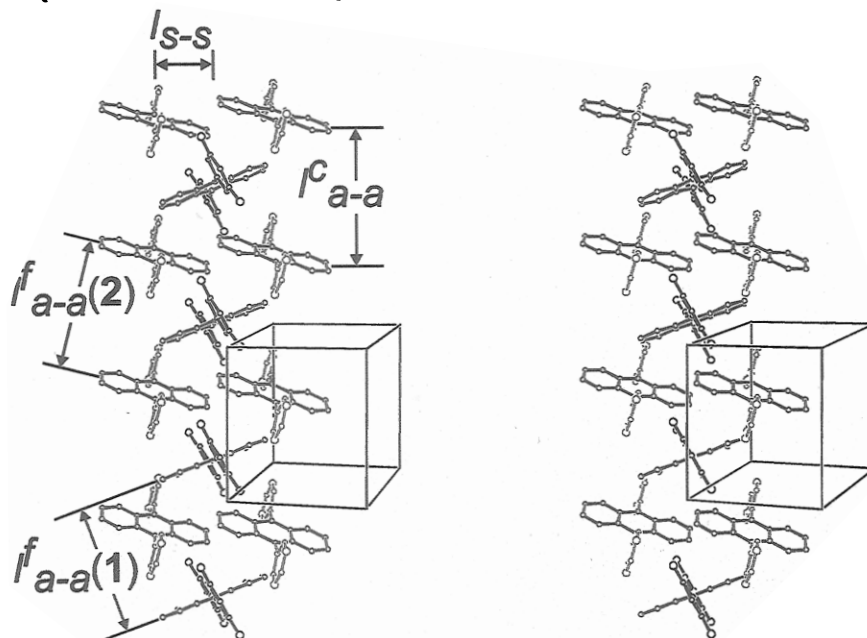


Figure 2. Arrangement of three neighboring molecular sheets in the crystal of adduct **1·2**: top view of the sheets (a) and side view in stereo of the three interpenetrating anthracene columns. Different colors have the same meanings as in Figure 1.

anthracene spacers to form columns. The present work is mainly concerned with three-dimensional (3D) structural control. A particular attention has been paid to the manipulation of the columns of anthracene (electron donor) and anthraquinone as well as guest quinones (electron acceptors) as models of functional aromatic moieties. Thus, we prepared bis(pyrimidine) derivatives of anthracene and anthraquinone (**2** and **3**, Scheme 1) as analogous orthogonal triads and determined the crystal structures of such adducts as **1·2**, **1·3**·C₆H₅OCH₃, **1·2**(benzoquinone), and **1·2**(anthraquinone). In the schematic representation of crystal structures hereafter, orthogonal aromatic triads **1–3** are simplified as structure **4** where X = OH or N and S = anthracene or anthraquinone. We report here on the importance of self-assembly of 1D chains or 2D sheets in the desired 3D control of aromatic columns.^{7–11}

(7) For recent reviews on the use of intermolecular interactions, especially hydrogen-bonding, to control crystal structures, see: (a) Lehn, J.-M. *Angew. Chem., Int. Ed. Engl.* **1988**, *27*, 89–112; **1990**, *29*, 1304–1319. (b) Mathias, J. P.; Stoddart, J. F. *Chem. Soc. Rev.* **1992**, *21*, 215–225. (c) Aakeröy, C. B.; Seddon, K. R. *Chem. Soc. Rev.* **1993**, *22*, 397–407. (d) Reference 5.

Results and Discussion

Structure of Adduct 1·2. Anthracene Columns Accompanied by Hydrogen-Bonded Resorcinol-Pyrimidine

(8) For the pattern and selectivity in forming hydrogen bonds from various functional groups, see: (a) Etter, M. C. *Acc. Chem. Res.* **1990**, *23*, 120–126. (b) Etter, M. C.; MacDonald, J. C.; Bernstein, J. *Acta Crystallogr.* **1990**, *B46*, 256–262. (c) Etter, M. C. *J. Phys. Chem.* **1991**, *95*, 4601–4610.

(9) For recent examples of the formation of ordered crystal structures involving hydrogen-bonded one-dimensional motifs (molecular *tapes* and *chains*), see: (a) Lehn, J.-M.; Mascal, M.; DeCian, A.; Fischer, J. *J. Chem. Soc., Chem. Commun.* **1990**, 479–481. (b) Etter, M. C.; Admond, D. A. *J. Chem. Soc., Chem. Commun.* **1990**, 589–591. (c) Zerkowski, J. A.; Seto, C. T.; Wierda, D. A.; Whitesides, G. M. *J. Am. Chem. Soc.* **1990**, *112*, 9025–9026. (d) G.-Tellado, F.; Geib, S. J.; Goswami, S.; Hamilton, A. D. *J. Am. Chem. Soc.* **1991**, *113*, 9265–9269. (e) Reference 7c. (f) Lehn, J.-M.; Mascal, M.; DeCian, A.; Fischer, J. *J. Chem. Soc., Perkin Trans. 2* **1992**, 461–467. (g) Zerkowski, J. A.; Seto, C. T.; Whitesides, G. M. *J. Am. Chem. Soc.* **1992**, *114*, 5473–5475. (h) Zerkowski, J. A.; MacDonald, J. C.; Seto, C. T.; Wierda, D. A.; Whitesides, G. M. *J. Am. Chem. Soc.* **1994**, *116*, 2382–2391. (i) Zerkowski, J. A.; Whitesides, G. M. *J. Am. Chem. Soc.* **1994**, *116*, 4298–4304. (j) Zerkowski, J. A.; Mathias, J. P.; Whitesides, G. M. *J. Am. Chem. Soc.* **1994**, *116*, 4305–4315. (k) Fan, E.; Vicent, C.; Geib, S. J.; Hamilton, A. D. *Chem. Mater.* **1994**, *6*, 1113–1117.

Table 1. Crystallographic Data and Important Distances and Angles^a

adduct	1·2(1BB) ^b	1·2	1·3·C ₆ H ₅ OCH ₃	1·2BQ	1·2AQ
crystal system	monoclinic	triclinic	triclinic	orthorhombic	triclinic
space group	<i>P2₁/n</i>	<i>P1</i>	<i>P1</i>	<i>Pnma</i>	<i>P1</i>
<i>a</i> , Å	9.534(6)	9.135(2)	11.096(2)	15.073(3)	8.250(2)
<i>b</i> , Å	13.479(4)	11.474(2)	12.379(5)	31.578(3)	9.536(2)
<i>c</i> , Å	15.572(4)	8.496(1)	9.499(2)	6.214(5)	13.362(2)
α, deg		94.549(8)	112.12(2)		77.61(2)
β, deg	100.77(5)	91.571(7)	100.43(2)		75.56(2)
γ, deg		92.266(1)	86.49(3)		73.34(2)
<i>V</i> , Å ³	1966.0	866.6(1)	1188.7(6)	2957.7(1)	952.5(6)
<i>Z</i>	2	1	1	4	1
<i>D_c</i> , g/cm ³	1.267	1.365	1.230	1.370	1.412
<i>R</i>	0.096	0.070	0.226 ^c	0.073	0.087
<i>R_w</i>	0.131	0.071		0.049	0.103
no. unique rflcn	4443	2637	3543	2575	3915
no. rflcn used ^d	2433	1766	2341	758	1903
<i>I</i> ^f _{a-a} , Å	12.22	8.49 (1) 8.40 (2)	11.78	3.99	5.24
<i>I</i> ^c _{a-a} , Å	13.48	9.14	12.38	6.21	8.25
<i>I</i> ^f _{q-q} , Å ^e			10.56	2.87	3.55 (1) 3.03 (2)
<i>I</i> ^c _{q-q} , Å ^e			12.38	6.21	4.45 (1) 3.80 (2)
<i>I</i> _{c-c} , Å	9.86	12.34 4.20 (c-c')	8.80 4.40 (a-q)	15.79 5.60 (a-q) 4.53 (q-q)	19.95 9.98 (a-q) 6.23 (a-q')
<i>I</i> _{s-s} , Å	7.40	3.77	6.02	7.54	5.46
θ, deg ^f	22.0	17.5 (1) 16.0 (2)	15.0 (1) 10.0 (3)	50.0 (1) 62.5 (BQ)	45.0 (1) 37.0 (AQ)
φ, deg ^f	12.0	13.0 (1) 17.0 (2)	10.0 (1) 30.0 (3)	0 (1) 0 (BQ)	26.0 (1) 3.0 (AQ)
<i>I</i> _{O-O} , Å ^g	2.78			2.74 (1) 2.89 (2)	2.79 (1) 2.84 (2)
<i>I</i> _{O-N} , Å ^g		2.79 (1) 2.80 (2)	2.82 (1) 2.73 (2)		

^a Definitions are as follows: *I*^f_{a-a}, face-to-face anthracene–anthracene distance; *I*^c_{a-a}, center-to-center anthracene–anthracene distance; *I*^f_{q-q}, face-to-face quinone–quinone distance; *I*^c_{q-q}, center-to-center quinone–quinone distance; *I*_{c-c}, column-to-column distance; *I*_{s-s}, sheet-to-sheet distance; θ and φ, tilt angles of the long and short axes, respectively, of the anthracene or anthraquinone ring with respect to the column axis (referring to structures **5** and **6** in Scheme 1); *I*_{O-O}, O–O distance for the hydrogen-bonded O–H···O moiety; *I*_{O-N}, O–N distance for the hydrogen-bonded O–H···N moiety. ^b 1BB = isobutyl benzoate. Crystal data for the adduct 1·2(guest) slightly depend on included guest molecules. Data for the isobutyl benzoate adduct 1·2(1BB) are shown here (ref 6b). ^c Poor *R* value are due to disorder of included anisole molecules. ^d *I* > 3σ(*I*). ^e Numbers 1 and 2 in parentheses refer to two types of quinone–quinone distances shown in Figure 8b. ^f The line bisecting the bonds C₁–C₂ and C₄–C₅ is taken as the “long” axis for BQ. ^g Numbers 1 and 2 in parentheses refer to two types of hydrogen bonds shown in Figure 1b, 3b, 5b, and 7b.

Alternate Chains. Compound **2** (Scheme 1) was prepared (supporting information) by the Pd^{II}-catalyzed cross-coupling

(10) For recent examples of the formation of ordered crystal structures involving hydrogen-bonded two-dimensional motifs (molecular sheets and layers), see: (a) Leiserowitz, L.; Schmidt, G. M. *J. Chem. Soc.* **1969**, A, 2372–2382. (b) Etter, M. C.; Frankenbach, G. M. *Chem. Mater.* **1989**, 1, 10–12. (c) Harris, K. D. M.; Hollingsworth, M. D. *Nature* **1989**, 341, 19. (d) Zhao, X.; Chang, Y.-L.; Fowler, F. W.; Lauher, J. W. *J. Am. Chem. Soc.* **1990**, 112, 6627–6634. (e) Stainton, N. M.; Harris, K. D. M.; Howie, R. A. *J. Chem. Soc., Chem. Commun.* **1991**, 1781–1784. (f) Ung, A. T.; Bishop, R.; Craig, D. C.; Dance, I. G.; Scudder, M. L. *J. Chem. Soc., Chem. Commun.* **1993**, 322–323. (g) Reddy, D. S.; Goud, B. S.; Panneerselvam, K.; Desiraju, G. R. *J. Chem. Soc., Chem. Commun.* **1993**, 663–664. (h) Harris, K. D. M.; Stainton, N. M.; Callan, A. M.; Howie, R. A. *J. Mater. Chem.* **1993**, 3, 947–952. (i) Chang, Y.-L.; West, M.-A.; Fowler, F. W.; Lauher, J. W. *J. Am. Chem. Soc.* **1993**, 115, 5991–6000. (j) Reference 6c. (k) Aakeröy, C. B.; Hitchcock, P. B. *J. Mater. Chem.* **1993**, 2, 1129–1135. (l) Hollingsworth, M. D.; Brown, M. E.; Santarsiero, B. D.; Huffman, J. C.; Goss, C. R. *Chem. Mater.* **1994**, 6, 1227–1244. (m) Russell, V. A.; Etter, M. C.; Ward, M. D. *J. Am. Chem. Soc.* **1994**, 116, 1941–1952.

(11) For recent examples of the formation of ordered crystal structures having hydrogen-bonded three-dimensional motifs (molecular cages) of the diamondoid lattices, see: (a) Ermer, O.; Eling, A. *Angew. Chem., Int. Ed. Engl.* **1988**, 27, 829–833. (b) Ermer, O. *J. Am. Chem. Soc.*, **1988**, 110, 3747–3754. (c) Ermer, O.; Lindenberg, L. *Helv. Chim. Acta* **1991**, 74, 825–877. (d) Ermer, O. *Adv. Mater.* **1991**, 3, 608–611. (e) Simard, M.; Su, D.; Wuest, J. D. *J. Am. Chem. Soc.* **1991**, 113, 4696–4698. (f) Copp, S. B.; Subramanian, S.; Zaworotko, M. J. *J. Am. Chem. Soc.* **1992**, 114, 8719–8720. (g) Reddy, D. S.; Craig, D. C.; Rae, A. D.; Desiraju, G. R. *J. Chem. Soc., Chem. Commun.* **1993**, 1737–1739. (h) Zaworotko, M. J. *J. Chem. Soc. Rev.* **1994**, 23, 283–288. (i) Ermer, O.; Eling, A. *J. Chem. Soc., Perkin Trans. 2* **1994**, 925–944.

of dibromoanthracene and trimethylstannylpyrimidine,¹² which was obtained by the Pd⁰-promoted stannylation of bromopyrimidine.¹³ Recrystallization of an equimolar mixture of bis(resorcinol) and bis(pyrimidine) derivatives **1** and **2** from anisole exclusively afforded 1:1 cocrystals **1·2** ($\nu_{\text{OH}} = 3200 \text{ cm}^{-1}$ as compared with $\nu_{\text{OH}} = 3350 \text{ cm}^{-1}$ for compound **1**) as pale yellow plates. Single-crystal X-ray diffraction for the adduct shows an extensive resorcinol–pyrimidine O–H···N hydrogen-bonded network with $\angle\text{O–H–N} = 143^\circ$ or 156° , respectively, for hydrogen bond 1 or 2 shown in Figure 1b; this leads to a molecular sheet containing hydrogen-bonded resorcinol–pyrimidine alternate copolymeric chains together with anthracene columns (Figures 1a, schematic representation where X = OH, Y = N, and S = S' = anthracene; 1b, actual structure); in the present paper, different rings are shown in different colors (anthracene in red, quinone as either spacer or guest in green, resorcinol in black, and pyrimidine in blue) and hydrogen bonds are represented in light blue. Otherwise, the sheet structure is similar to that of homotopic hydrogen-bonded crystals **1**;⁶ (1) the anthracene ring is orthogonal with the resorcinol (in **1**) or pyrimidine (in **2**) ring, (2) hydrogen-bonded resorcinol and pyrimidine moieties are not coplanar but zigzag-arranged, and (3) all the anthracene rings along a column are parallel but not

(12) Cf. Azizian, H.; Eaborn, C.; Pidcock, A. *J. Organomet. Chem.* **1981**, 215, 49–58.

(13) Cf. Bailey, T. R. *Tetrahedron Lett.* **1986**, 27, 4407–4410.

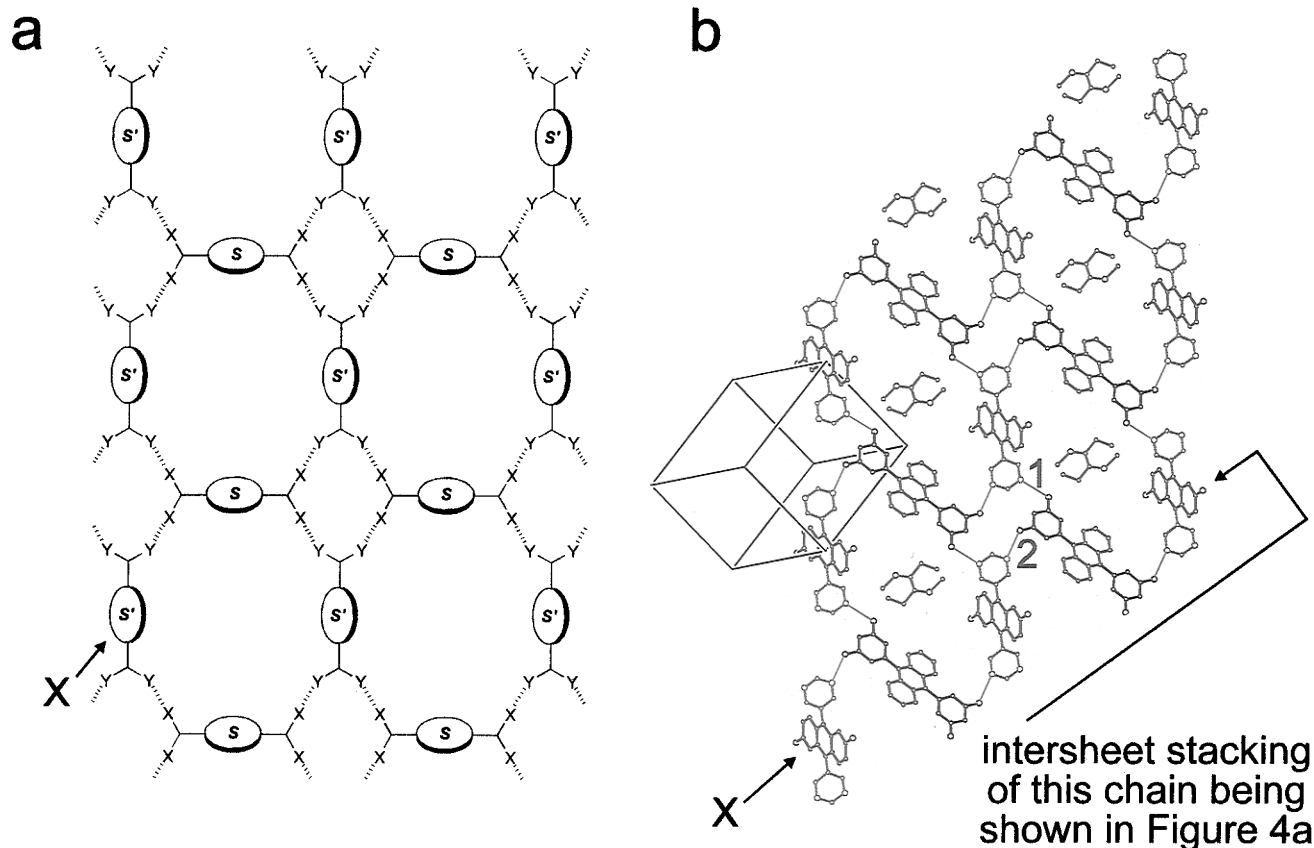


Figure 3. Structure of the hydrogen-bonded network in a molecular sheet in the crystal of adduct $1 \cdot 3 \cdot C_6H_5OCH_3$: schematic representation (a) and actual structure (b), where anthracene, anthraquinone, resorcinol, and pyrimidine rings are shown in red, green, black, and blue, respectively, and hydrogen bonds are in light blue. Pink-colored molecules in the cavities represent orientation-disordered anisole.

perpendicular with respect to the molecular sheet. In Table 1 are shown the crystallographic data as well as important distances, defined in Figures 1 and 2, such as center-to-center and face-to-face anthracene–anthracene distances I_{c-a}^c and I_{a-a}^f , intercolumn and intersheet distances I_{c-c} and I_{s-s} , and hydrogen-bond distances I_{O-O} and I_{O-N} in addition to the tilt angles θ and φ of the long and short axes of the anthracene rings with respect to the column axis (refer to structures **5** and **6** in Scheme 1).¹⁴ The crystal data for adduct $1 \cdot 2$ (guest) depend on the included guest molecules.⁶ Those for the isobutyl benzoate (IBB) adduct $1 \cdot 2$ (IBB)^{6b} are included in Table 1.

The nitrogen atoms which form an O–H···N hydrogen bond in adduct **1**·**2** are in the six-membered pyrimidine rings, in marked contrast to the exocyclic O–H···O hydrogen bonds in adduct $1 \cdot 2$ (IBB). This results in significant shortening (~ 4 Å) in I_{a-a}^f and I_{c-a}^c in the former adduct as compared with those in the latter. Interface distances of aromatic columns are thus controllable by a choice of accompanying interaction chains.

Another and more important difference in the two adducts lies in the ways as to how their large supramolecular cavities are filled. Recrystallization of compound **1** as host affords **1**–solvent adducts with a 1:2 stoichiometry in most cases.^{6b,c} The two solvent molecules as guests are incorporated in each cavity via hydrogen bonding (O–H···O–H···O–guest) between a pair of hydrogen-bonded OH groups of the host (O–H···O–H) and the oxygen atom of the guest (O–guest). In the present case, however, the O–H···N hydrogen bonds leave no free proton available for guest binding; there is no solvent incorporation as a consequence. Under these circumstances, the cavities in Figure 1 are partially filled via interpenetration of the

anthracene moieties between neighboring sheets, as shown in the top view (Figure 2a) of three neighboring sheets. The intersheet distance of $I_{s-s} = 3.77$ Å in adduct **1**·**2** may be compared with $I_{s-s} = 7.40$ Å in adduct $1 \cdot 2$ (IBB). Thus, the anthracene columns in neighboring sheets (A and A' in Figure 2a) are closely arranged and overlapped with $I_{c-c'} = 4.20$ Å, although two adjacent columns in a sheet (A and A in Figure 2a) are separated by a resorcinol–pyrimidine chain with $I_{c-c} = 12.34$ Å and must be *insulated* from each other. The side view of three columns in proximity indicated in Figure 2a is shown in Figure 2b in stereo.

Structure of Adduct $1 \cdot 3 \cdot C_6H_5OCH_3$. Concurrent Formation of Anthracene and Anthraquinone Columns. Compound **3** (Scheme 1) was prepared in a similar manner as above (supporting information). The combination of anthracene–resorcinol and anthraquinone–pyrimidine derivatives **1** and **3** provides an interesting case which may lead to either mixed (heterosoric) or segregated (homosoric) columns of the two different spacers.¹⁵ Recrystallization of an equimolar mixture of **1** and **3** from anisole afforded 1:1 cocrystals containing one molecule of the solvent, i.e., $1 \cdot 3 \cdot C_6H_5OCH_3$ as yellow prisms. The IR spectrum indicated a shift (150 cm^{-1}) in ν_{O-H} for **1** as above, while $\nu_{C=O}$ for **3** remained unchanged upon adduct formation. These results suggested an O–H···N hydrogen-bonding interaction as in adduct **1**·**2**. We first expected a 2D heterotopic hydrogen-bonded network (Figure 1a; X = OH, Y = N, S = anthracene, and S' = anthraquinone) analogous to that found for adduct **1**·**2**. This was, however, not the case.

(14) The plane containing a column axis and the long axes of anthracene moieties associated with the column is nearly perpendicular with the molecular sheet in every case.

(15) Simple charge-transfer complexes between π -donors and π -acceptors tend to form heterosoric columns having an alternate arrangement of donor and acceptor. For the structure of anthracene–TCNQ adduct (TCNQ = tetracyanoquinodimethane), see: Williams, R. M.; Wallwork, S. C. *Acta Crystallogr.* **1968**, B24, 168–174. However, some charge-transfer salts form homosoric donor columns and acceptor columns; ref 3b, Chapter 3.

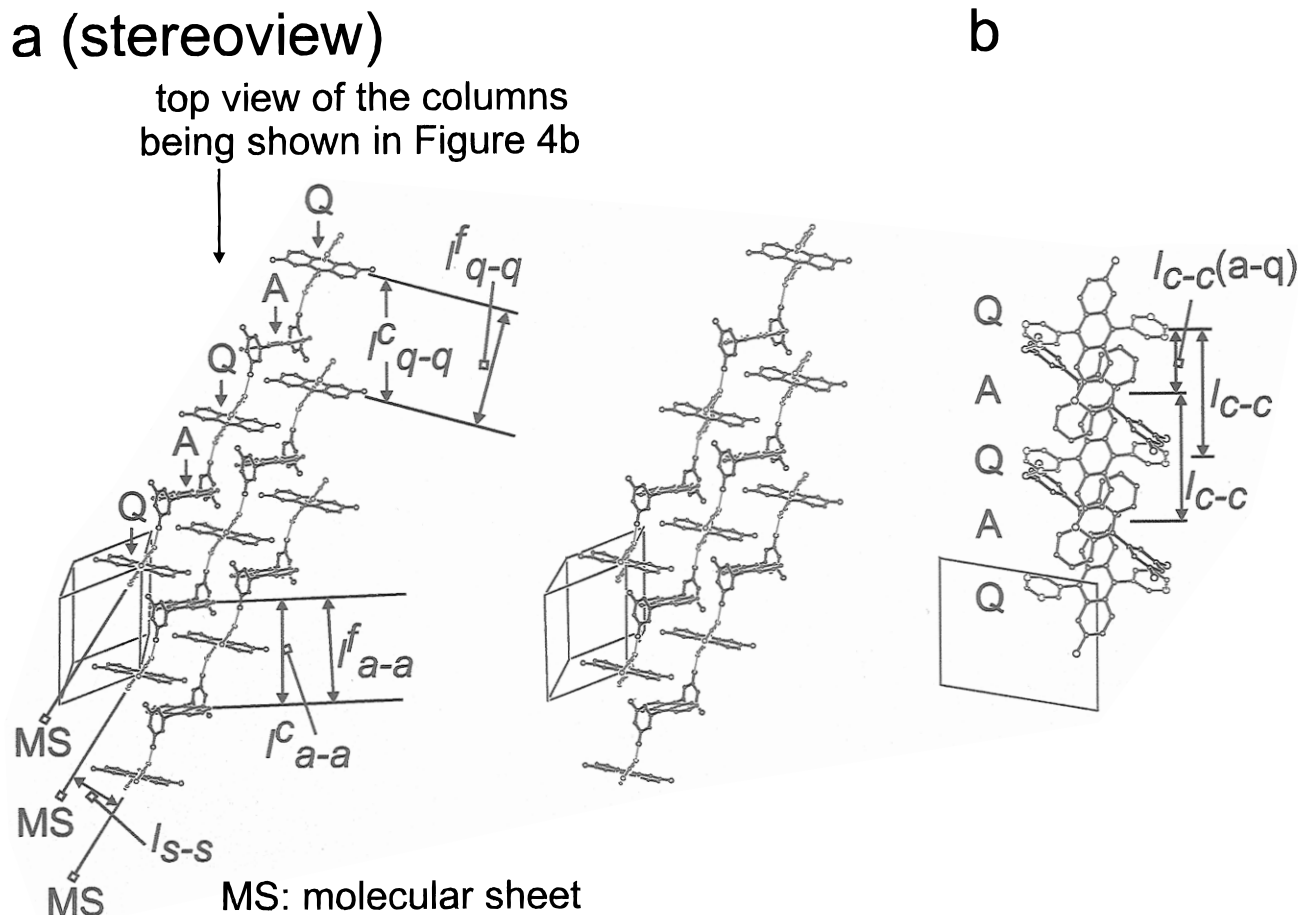


Figure 4. Arrangement of three neighboring molecular sheets in the crystal of adduct $1 \cdot 3 \cdot C_6H_5OCH_3$: intersheet stacking of the anthracene (A) and anthraquinone (Q) moieties to form columns (a, in stereo) and top view of the five neighboring columns shown in Figure 4a (b). Different colors have the same meanings as in Figure 3.

X-ray diffraction for adduct $1 \cdot 3 \cdot C_6H_5OCH_3$ confirmed the following characteristic aspects in reference to Figure 3. (1) The resorcinol and pyrimidine moieties exclusively form $O-H \cdots N$ hydrogen bonds with $\angle O-H-N = 154^\circ$ or 135° , respectively, for hydrogen bond 1 or 2 in Figure 3b; there is neither resorcinol–resorcinol nor resorcinol–quinone $O-H \cdots O$ hydrogen bond. (2) The hydrogen-bonded network in the resulting sheet is in such a way as to give cyclic arrays of two resorcinol and two pyrimidine rings as well as large cavities composed of two molecules of both **1** and **3**; this is in marked contrast to the resorcinol–pyrimidine alternate linear copolymeric chains in adduct **1·2** (Figure 1). (3) Each cavity incorporates one molecule of orientation-disordered solvent anisole. (4) There is no well-defined aromatic stack column in a sheet. The anthracene and anthraquinone rings along the direction of arrow X in Figure 3 are far from parallel to each other. (5) The molecular sheets, on the other hand, are layered in such a way as to give intersheet columns for both the anthracene (A) and anthraquinone (Q) spacers, as shown in Figure 4a in stereo for three neighboring sheets (MS); each chain shown by MS represents an anthracene–anthraquinone alternate chain in the direction of arrow X in Figure 3b. The segregated anthracene and anthraquinone columns are kept in proximity with $I_{c-c(a-q)} = 4.40 \text{ \AA}$ and partially overlapped with each other as shown in the top view (Figure 4b) of five columns. (6) Thus, the designed $O-H \cdots N$ hydrogen-bonded network prevents otherwise potential charge-transfer¹⁵ (with anthracene and/or resorcinol rings) and/or hydrogen-bonding (with resorcinol ring) interactions involving the quinone moiety of **3**. It is well-known that quinones and polyphenols including resorcinol readily form hydrogen-bonded/charge-transfer complexes of the quinhydrone type.¹⁶

Structure of Adduct 1·2(1,4-Benzoquinone). Intersheet Anthracene and Quinone Columns Maintained by Polycatenated Hydrogen-Bond Network. An extensive 2D network may also be achieved by using a bifunctional bridging agent (B) such as *p*-quinones, as schematically shown in Figure 5a. Slow penetration of hexane into a solution of compound **1** and 10 equiv of 1,4-benzoquinone (BQ) in ethyl acetate gave single crystals of a 1:2 adduct **1·2BQ**, without solvent incorporation, as red needles. The $\nu_{C=O}$ values for BQ shifted from 1679 to 1650 cm^{-1} upon adduct formation. X-ray diffraction revealed the following aspects. (1) Compound **1** and the quinone indeed form an expected hydrogen-bond network to give a sheet, as schematically shown in Figure 5a ($X = OH$, $B = BQ$, and $S = anthracene$). The structure of a hydrogen-bonded cyclic array composed of four molecules of both **1** and BQ is shown in Figure 5b. (2) Three such sheets overlap with each other on the same plane to give a triply-interpenetrated or polycatenated¹⁷ supramolecular sheet, as shown in Figure 6 in stereo. Large cavities in Figure 5 are filled in this way, and both the anthracene (A) and BQ (Q) rings are packed vertically to form segregated columns having a small I^f_{a-a} (3.99 \AA) or I^f_{q-q} (2.87 \AA) value; they are, however, highly slided/tilted as indicated by the large

(16) (a) Bernstein, J.; Cohen, M. D.; Leiserowitz, L. *The Chemistry of the Quinonoid Compounds*; Patai, S., Ed.; Interscience: New York, 1974; pp 94–99. (b) Desiraju, G. R.; Curtin, D. Y.; Paul, I. C. *Mol. Cryst. Liq. Cryst.* **1979**, *52*, 563–570. (c) Depew, M. C.; Wan, J. K. S. *The Chemistry of the Quinonoid Compounds*; Patai, S., Rappoport, Z., Eds.; Wiley: Chichester, 1988; Vol. 2, Part 2, pp 965–968.

(17) (a) Bitsch, F.; D.-Buchecker, C. O.; Khémis, A.-K.; Sauvage, J.-P.; Dorselaer, A. V. *J. Am. Chem. Soc.* **1991**, *113*, 4023–4025. (b) D.-Buchecker, C.; Frommberger, B.; Lüer, I.; Sauvage, J.-P.; Vögtle, F. *Angew. Chem., Int. Ed. Engl.* **1993**, *32*, 1434–1437. (c) Amabilino, D. B.; Ashton, P. R.; Reder, A. S.; Spencer, N.; Stoddart, J. F. *Angew. Chem., Int. Ed. Engl.* **1994**, *33*, 433–437.

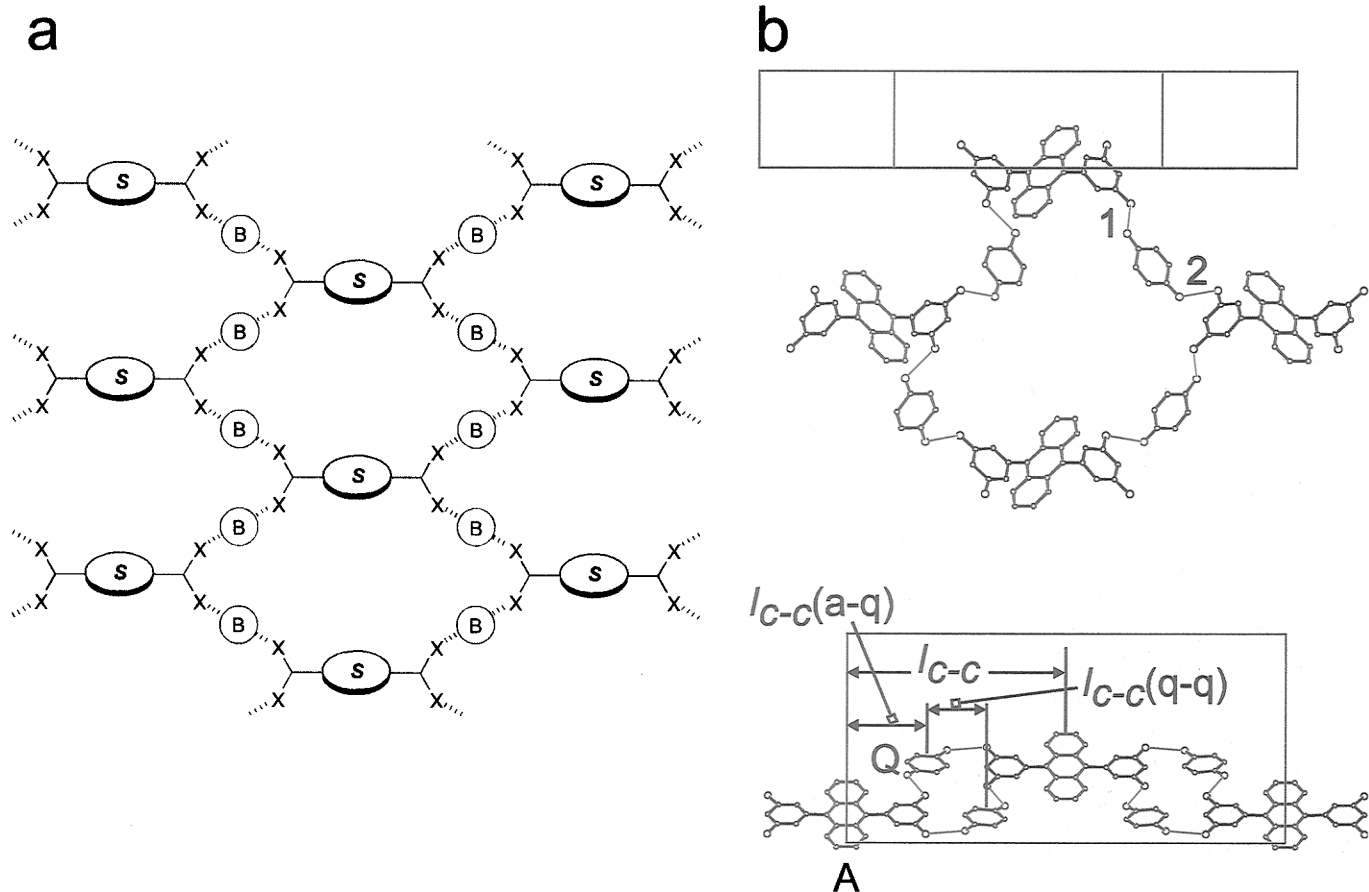


Figure 5. Structure of the hydrogen-bonded network in a molecular sheet in the crystal of adduct **1**·2(BQ): schematic representation (a, where B is BQ), actual structure of a hydrogen-bonded cyclic array of four molecules of both **1** and BQ (b), and top view of Figure 5b (c). Anthracene, BQ, and resorcinol rings are shown in red, green, and black, respectively, and hydrogen bonds are in light blue.

(stereoview)

top view of the columns
being shown in Figure 5c

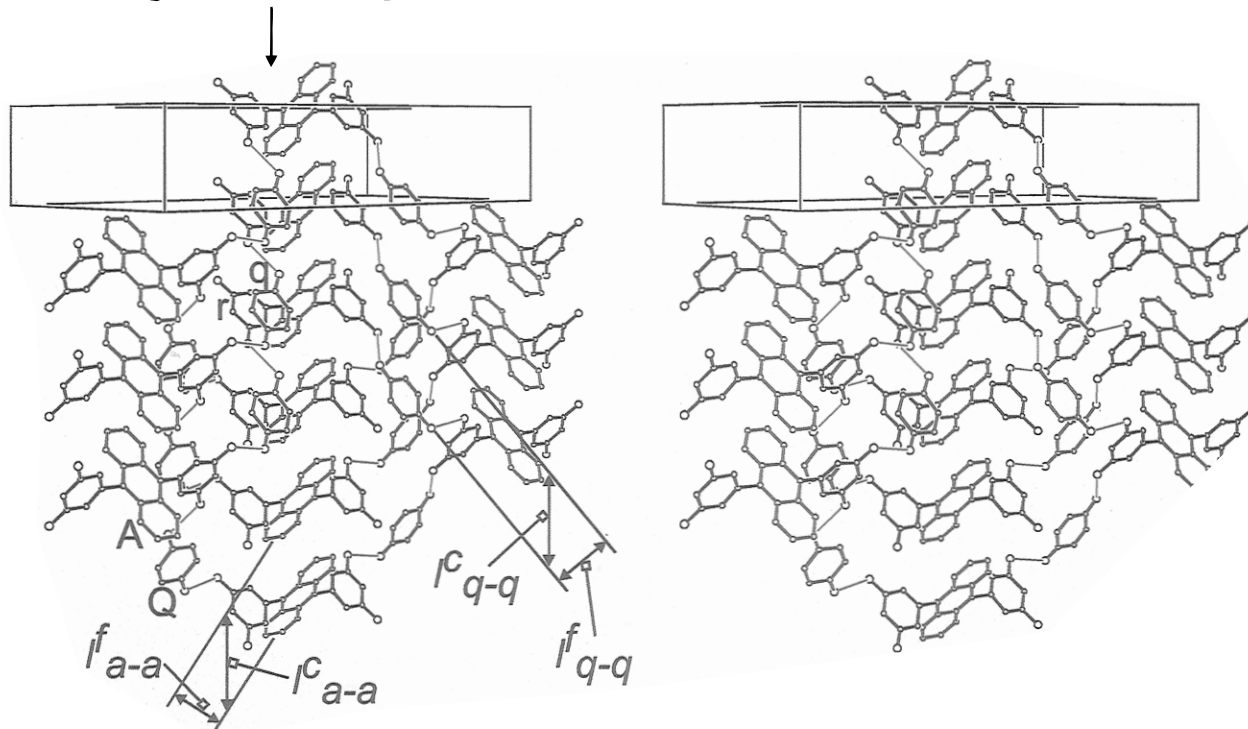


Figure 6. Stereoview of the three-fold interpenetration or polycatenation of the hydrogen-bonded network shown in Figure 5b. Different colors have the same meanings as in Figure 5.

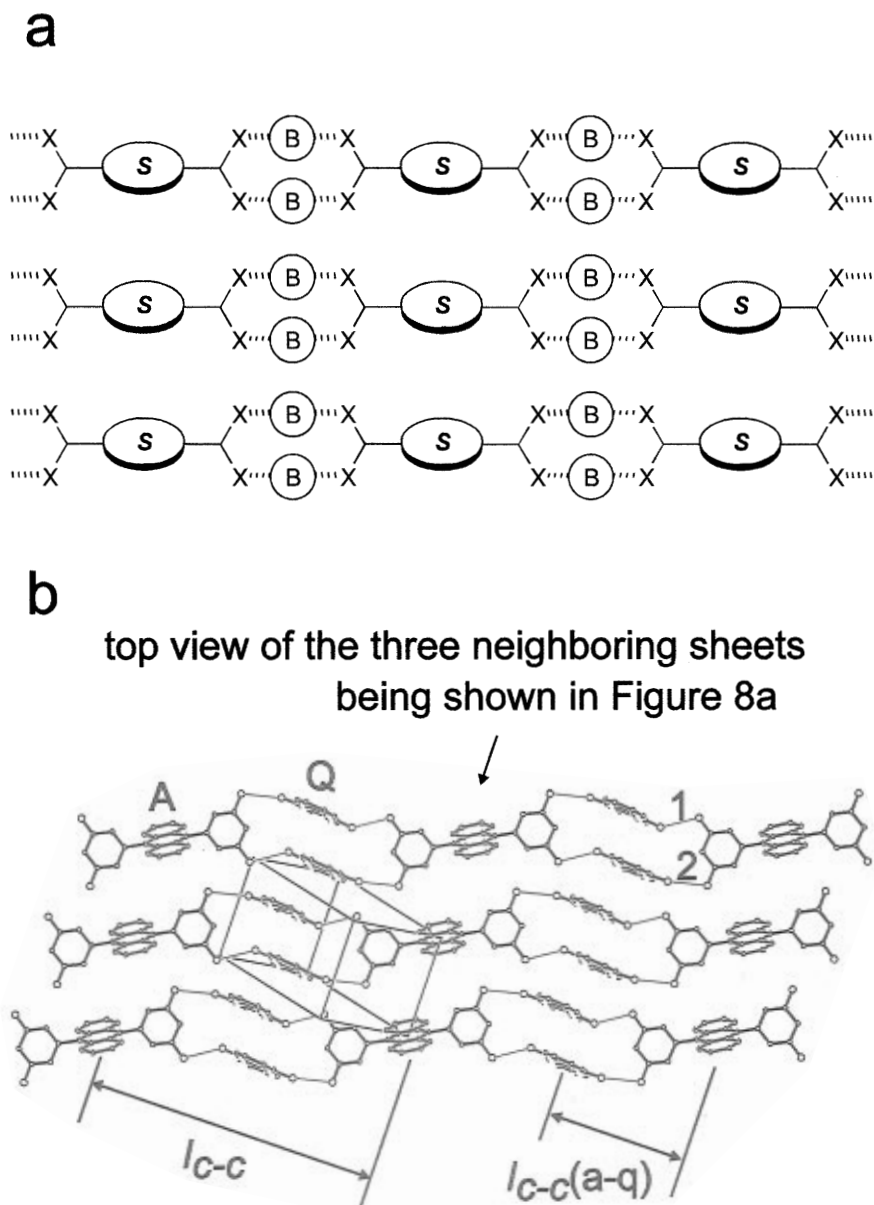


Figure 7. Vertical stacking of the hydrogen-bonded chains in the crystal of adduct **1·2AQ**: schematic representation (a, where B is AQ) and actual structure (b), where anthracene, AQ, and resorcinol rings are shown in red, green, and black, respectively, and hydrogen bonds are in light blue.

tilt angles θ (Table 1). The top view of the columns in Figure 6 is shown in Figure 5c. (3) The anthracene and BQ rings are either far apart or almost perpendicular with each other; there seems to be no charge-transfer (CT) interaction between them. (4) The resorcinol (r) and the quinone (q) rings not hydrogen-bonded are roughly parallel and partially overlapped with $I_{r-q}^f \approx 3 \text{ \AA}$ (Figure 6), a distance which may be short enough to allow a CT interaction. This interaction is plausibly responsible for the red coloration of adduct **1·2BQ** ($\lambda_{\text{max}} = 510 \text{ nm}$ in the solid state). In view of the importance of charge-transfer/hydrogen-bonding interactions between quinone and polyphenol (resorcinol), the present adduct can be regarded as an analogue of quinhydrones.¹⁶

Structure of Adduct 1·2(9,10-Anthraquinone). Interchain and Intersheet Control of Segregated Anthracene and Anthraquinone Columns. Slow evaporation of a diethyl ether solution of an equimolar amount of compound **1** and 9,10-anthraquinone (AQ) gave single crystals of 1:2 adduct **1·2AQ** as red plates; $\nu_{\text{C=O}} = 1670 \text{ cm}^{-1}$ as compared with $\nu_{\text{C=O}} = 1679 \text{ cm}^{-1}$ for AQ alone. The crystal structure for adduct **1·2AQ** turned out to be quite different from that of adduct **1·2BQ**. (1) Compound **1** and a *face-to-face stacked dimer* of

AQ form a hydrogen-bonded alternate copolymeric chain (Figure 7; X = OH, B = AQ, and S = anthracene). (2) The polymeric chains pack vertically to give anthracene (A) and anthraquinone (Q) columns, which are separated by the resorcinol chain with $I_{c-c(a-q)} = 9.98 \text{ \AA}$ in reference to Figure 7b. (3) The resulting supramolecular sheets themselves pack laterally to give a close proximity or even a partial overlap of the anthracene (A) and anthraquinone (Q') columns with $I_{c-c(a-q')} = 6.23 \text{ \AA}$, as shown in the top view (Figure 8a) of three neighboring sheets and the side view (Figure 8b, in stereo) of a pair of A and Q' columns.

In marked contrast to the case of adduct **1·2BQ**, the quinone ring is almost completely perpendicular with respect to the resorcinol ring in **1** (Figure 8b); there must be no CT interaction between them. Adduct **1·2AQ** is highly red-colored ($\lambda_{\text{max}} = 540 \text{ nm}$ in the solid state). This coloration may arise from some kind of CT interaction between anthracene (A) donor columns and anthraquinone (Q') acceptor columns. Such an interaction between donor and acceptor columns is particularly interesting in view of highly conducting CT salts characterized by segregated donor and acceptor columns.⁴

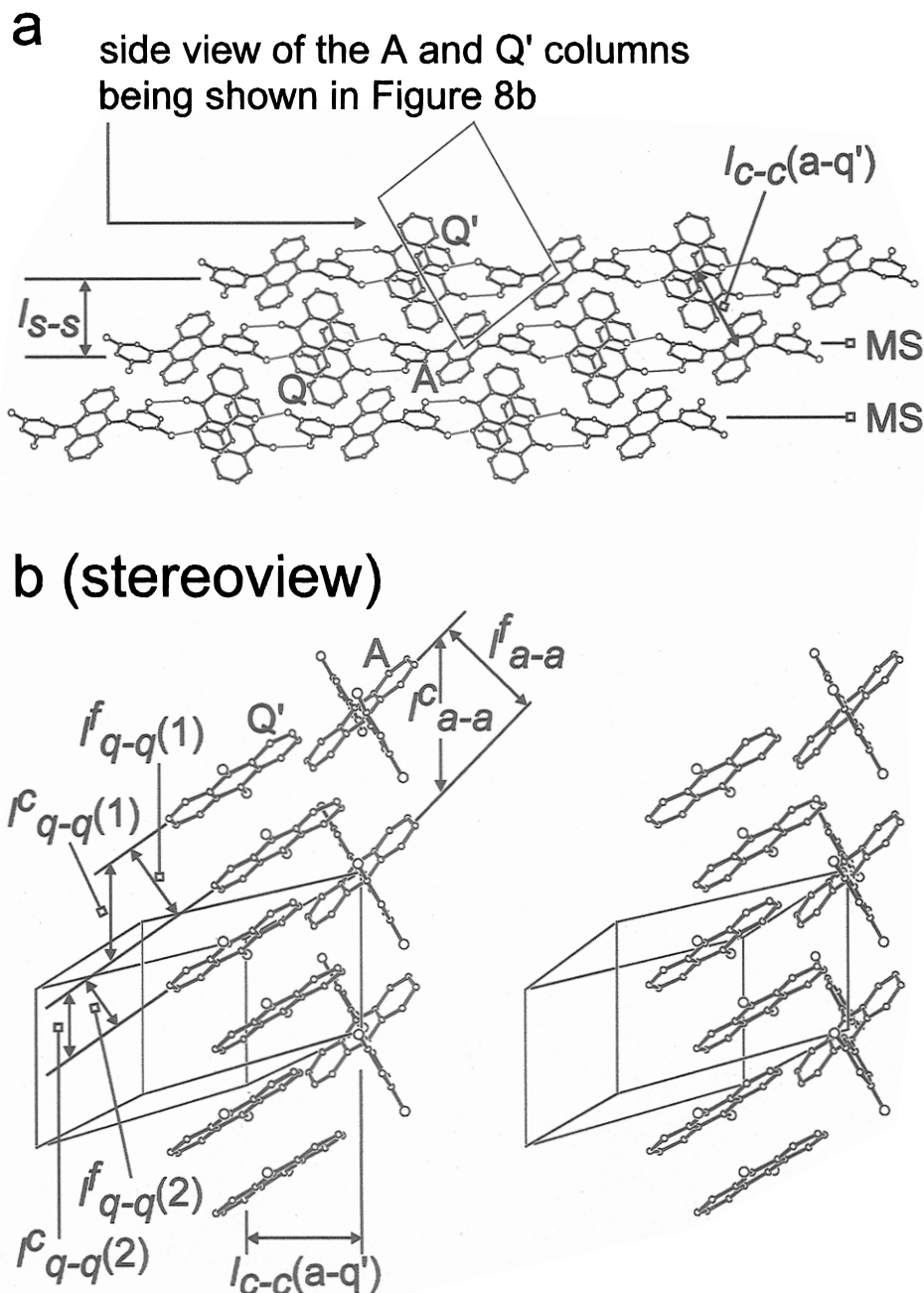


Figure 8. Arrangement of three neighboring molecular sheets in the crystal of adduct **1**·2AQ: top view of the sheets (a) and side view of two neighboring anthracene (A) and anthraquinone (Q') columns in different sheets (b, in stereo). Different colors have the same meanings as in Figure 7.

Concluding Remarks

All the crystals investigated here exhibit an extensive hydrogen-bonded network; the four interaction sites X in triads **1**–**3** and the two carbonyl groups in quinones BQ and AQ as guests are involved in hydrogen bonding. However, the network topologies are still highly sensitive to slight changes in molecular structures; otherwise closely related compounds such as **2** and **3** or BQ and AQ give rise to quite different crystal structures when cocrystallized with compound **1** under otherwise identical conditions.

All the adducts show a strong tendency to form columns, many of which are constructed via self-assembly of 1D (in adduct **1**·2AQ) or 2D (in adducts **1**·**3** and **1**·2BQ) networks. Packing of 1D chains or 2D sheets would be much simpler than that of single molecules of the 3D character and may even be designable. Most importantly, 3D control of different columns, i.e., co-alignment in proximity of donor and acceptor columns, can also be achieved in this manner, as typically demonstrated

by the behavior of adduct **1**·2AQ as a red-colored anthracene-anthraquinone charge-transfer molecular-crystal. The *network-self-assembly strategy* thus provides a general method to balance intermolecular interaction and crystal packing; *design interaction polymers (chains or sheets) and let them self-assemble*.

Further work is now under way along three lines: (1) physicochemical characterization of the present adducts, (2) use of potential electron-donors such as porphyrins and S- or Se-heterocycles as aromatic spacers in place of anthracene, and (3) use of various orthogonal systems as interaction sites in place of the resorcinol or pyrimidine ring.

Acknowledgment. This work was supported by the grant-in-aids for Y.A. from the Ministry of Education, Science, and Culture of the Japanese Government.

Supporting Information Available: Experimental Section with headings of General Procedures, 9,10-Bis(5-pyrimidinyl)-anthracene (**2**), 9,10-Bis(5-pyrimidinyl)-2,6-anthraquinone (**3**),

Recrystallization, and X-ray Crystal Structure Determinations and crystal structural data including tables of atomic coordinates, anisotropic thermal parameters, bond lengths and angles, and torsion angles for adducts **1**•**2**, **1**•**3**•C₆H₅OCH₃, **1**•**2**BQ, and **1**•**2**AQ (32 pages). This material is contained in many libraries

on microfiche, immediately follows this article in the microfilm version of the journal, can be ordered from the ACS, and can be downloaded from the Internet; see any current masthead page for ordering information and Internet access instructions.

JA953600K